

2007

Toward automatic measurement of the linewidth-enhancement factor using optical feedback self-mixing interferometry with weak optical feedback

Yanguang Yu

Zhengzhou University, yanguang@uow.edu.au

Jiangtao Xi

University of Wollongong, jiangtao@uow.edu.au

Joe F. Chicharo

University of Wollongong, chicharo@uow.edu.au

Thierry Bosch

ENSEEIHT, France

Follow this and additional works at: <https://ro.uow.edu.au/infopapers>



Part of the [Physical Sciences and Mathematics Commons](#)

Recommended Citation

Yu, Yanguang; Xi, Jiangtao; Chicharo, Joe F.; and Bosch, Thierry: Toward automatic measurement of the linewidth-enhancement factor using optical feedback self-mixing interferometry with weak optical feedback 2007.

<https://ro.uow.edu.au/infopapers/3057>

Toward automatic measurement of the linewidth-enhancement factor using optical feedback self-mixing interferometry with weak optical feedback

Abstract

This paper proposes an approach for automatically measuring the linewidth-enhancement factor (LEF) of semiconductor lasers using optical feedback self-mixing interferometry (OFSMI), which works in weak optical feedback regime and where the external target is subject to simple harmonic vibration with unknown vibration frequency and magnitude. According to well-known Lang–Kobayashi theory the waveform of the modulated optical output power from the OFSMI system is influenced by multiple parameters, including the LEF, the optical feedback level factor, and the parameters related to the movement of external target. In order to estimate LEF, other parameters must also be considered and, hence, a multiple parameter estimation strategy is required. We propose a solution for this multiple parameter estimation problem based on the principle of data-to-theoretical model match. In particular, a strategy for minimizing a cost function in order to achieve the best fitting is proposed with which all the unknown parameters can be estimated. The performance of the proposed approach is tested using experimental data in comparison with other two approaches. It is seen that, over different experimental signals, the standard deviation for estimated LEF is less than 4.58% on average, which shows that results have excellent consistency. Moreover, the proposed approach also provides a solution for vibration measurement (that is, vibration frequency and magnitude).

Disciplines

Physical Sciences and Mathematics

Publication Details

Yu, Y., Xi, J., Chicharo, J. F. & Bosch, T. (2007). Toward automatic measurement of the linewidth-enhancement factor using optical feedback self-mixing interferometry with weak optical feedback. *IEEE Journal of Quantum Electronics*, 43 (7), 527-534.

Toward Automatic Measurement of the Linewidth-Enhancement Factor Using Optical Feedback Self-Mixing Interferometry With Weak Optical Feedback

Yanguang Yu, Jiangtao Xi, *Senior Member, IEEE*, Joe F. Chicharo, *Senior Member, IEEE*, and Thierry Bosch, *Senior Member, IEEE*

Abstract—This paper proposes an approach for automatically measuring the linewidth-enhancement factor (LEF) of semiconductor lasers using optical feedback self-mixing interferometry (OFSMI), which works in weak optical feedback regime and where the external target is subject to simple harmonic vibration with unknown vibration frequency and magnitude. According to well-known Lang–Kobayashi theory the waveform of the modulated optical output power from the OFSMI system is influenced by multiple parameters, including the LEF, the optical feedback level factor, and the parameters related to the movement of external target. In order to estimate LEF, other parameters must also be considered and, hence, a multiple parameter estimation strategy is required. We propose a solution for this multiple parameter estimation problem based on the principle of data-to-theoretical model match. In particular, a strategy for minimizing a cost function in order to achieve the best fitting is proposed with which all the unknown parameters can be estimated. The performance of the proposed approach is tested using experimental data in comparison with other two approaches. It is seen that, over different experimental signals, the standard deviation for estimated LEF is less than 4.58% on average, which shows that results have excellent consistency. Moreover, the proposed approach also provides a solution for vibration measurement (that is, vibration frequency and magnitude)

Index Terms—Fitting algorithm, linewidth-enhancement factor (LEF), optical feedback interferometry, self-mixing effect, semiconductor laser.

I. INTRODUCTION

THE linewidth-enhancement factor (LEF) is a fundamental parameter of semiconductor lasers (SLs) that characterizes the characteristics of SLs, such as the linewidth, the chirp, the injection lock range and the dynamic performances. Since the LEF was proposed in the early 1980s [1], [2], extensive research work

has been carried out to study this parameter [3]–[6] and various techniques have been developed to measure its value, such as the approach using amplified spontaneous emission (ASE) spectroscopy [7], the method based on radio-frequency (RF) modulation [8], the technique using injection locking [9], [10], and the measurements based on optical feedback or optical feedback self-mixing interferometric (OFSMI) phenomenon [11]–[13]. Among existing techniques, the approaches using OFSMI are characterized by an apparent ease of implementation and simplicity in system structure.

The OFSMI effect refers to a phenomenon that occurs when a small fraction of the light emitted by a SL is backscattered or reflected by an external target and re-enters the laser active cavity. As the target forms an external cavity for the laser, when it moves along the light beam, a variance in the emitted laser power can be observed, which is referred to as an OFSMI signal. The OFSMI signals were found to contain information about the external target as well as the SL, and various sensing applications based on OFSMI effect have been proposed [14]–[16].

The idea of determining the LEF based on the OFSMI signal comes from [17], where it was suggested that the LEF can be estimated using an OFSMI system by comparing the observed laser intensity and the theoretical one.

However, [17] did not specify how to perform the comparison. More recently, Yu *et al.* [12] developed a theoretical relationship between the OFSMI fringes and the LEF by making use of the hysteresis in the OFSMI signal at the moderate feedback regime. The proposed approach [12] is attractive as it does not need RF or optical spectrum measurements. However, its usage and performance are limited by the restrictions as follows. First, the OFSMI waveforms must have zero-crossing points, which then require that optical feedback level (measured by parameter C) falls within a small range. For example, when LEF is between 3 and 5, C must be within $1 < C < 3$. The range is even narrower for smaller LEF, and accordingly, the optical feedback must be carefully adjusted. Consequently, application of the approach in [12] is limited as it is difficult for some lasers to achieve moderate optical feedback. Second, the external target must move away from and back to the laser facet at a constant speed, which is also difficult in practice. In [12], the experimental setup uses an external target vibrating simple harmonically, which obviously does not exhibit a constant speed at any time instance. As a result, the approach has an inherent error

Manuscript received July 6, 2006; revised February 8, 2007. This work was supported in part by Australian Research Council on ARC Linkage International Award Project LX0561454 and in part by the National Natural Science Foundation of China (NSFC) under Project 60574098.

Y. Yu is with College of Information Engineering, Zhengzhou University, Zhengzhou 450052, China (e-mail: yanguangyu@zzu.edu.cn).

J. Xi and J. F. Chicharo are with School of Electrical Computer and Telecommunications Engineering, University of Wollongong, Wollongong NSW 2522, Australia (e-mail: Jiangtao@uow.edu.au; chicharo@uow.edu.cn).

T. Bosch is with Ecole Nationale Supérieure d'Electrotechnique, d'Electronique, d'Informatique, d'Hydraulique et des Télécommunications (ENSEEIH), F 31071 Toulouse Cedex 7, France (e-mail: Thierry.Bosch@enseiht.fr).

Digital Object Identifier 10.1109/JQE.2007.897862

in terms of measurement. In order to reduce the error, it is suggested in [12] that the two fringes used are chosen at the point in time when the external target moves across the equilibrium position, where it has the minimum acceleration and the movement trace is most linear.

For LEF measurement, we always want the OFSMI-based setup to be able to measure most (if not all) types of lasers. As the approach in [12] is not applicable for some situations, we should seek an alternative approach for achieving the measurement. Considering that weak optical feedback is easy to achieve with most types of lasers, it is useful to develop an approach that works for this particular situation. This issue was addressed in [13] with an approach based on a data fitting paradigm whereby the theoretical model incorporates an estimate of the LEF and C that are optimized to yield the best match for the observed OFSMI data. The approach in [13] does not require that external target moves with a constant speed and, hence, it does not suffer from the inherent error due to the nonuniform movement speed of the external target. Besides, as segments of OFSMI signal data samples are employed, the resulting measurement by the approach in [13] is more robust and immunized to noise. Unfortunately, the approach proposed in [13] assumes that a movement trace of the external target is known *a priori*. This is a tough requirement as a complex mechanic system is usually needed for achieving a particular motion for the external target. Even if such a particular motion can be achieved and implemented, it is still difficult to measure LEF using the approach in [13]. The reason is that the OFSMI signal waveform is dependent on the movement trace of the point on the external target where the laser beam is reflected. Based on our experience, the point varies when there is a slight change in the system setup and, hence, it is almost impossible to add an extra setup to the OFSMI system in order to track the point and measure the vibration of the point in real-time.

In this paper we propose to achieve automatic, accurate and robust measurement of the LEF using an OFSMI system with weak feedback. In particular, the proposed approach is still based on the principle of best data-to-model fitting and hence it keeps the advantage of the approach proposed in [13], but the exact movement trace of the external target is not required, which will significantly reduce the work and cost associated with system calibration and maintenance.

Estimation of LEF under the above conditions is in fact a multiple parameter estimation problem, as the parameters influencing the OFSMI signal waveform include not only the LEF and C , but also those associated with the movement of the external target according to Lang–Kobayashi theory. We should not simply evaluate the LEF regardless of other parameters. However, multiple parameter estimation is a challenging task as the unknown parameters are coupled together in terms of their influence on the OFSMI signals. In this paper we will propose an optimized strategy to carry out the multiple parameter estimation.

This paper is organized as follows. The system setup and a basic theoretical model are presented in Section II, in which all parameters influencing the OFSMI signal are described. Section III presents the algorithms for performing vibration frequency determination, rough estimation of vibration amplitude,

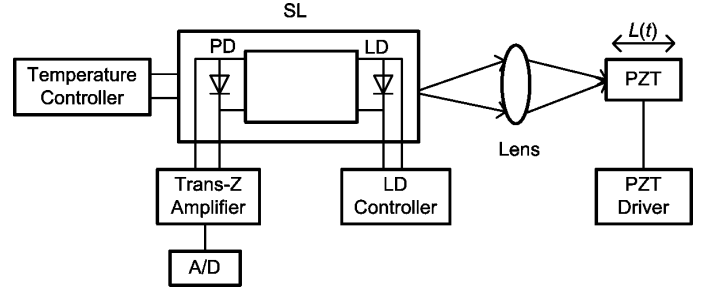


Fig. 1. Experimental setup used for obtaining OFSMI signals.

and automatic data segmentation. In Sections IV and V, the data-fitting principle with a cost function for multiple parameter estimation is proposed and an optimization strategy based on the analysis of the cost function is developed. Then in Section VI the performance of the proposed approach is tested using experimental data in comparison with existing approaches. Finally, Section VII concludes the paper.

II. SYSTEM SETUP AND THEORETICAL MODEL

In this paper we use an OFSMI experimental setup shown in Fig. 1, which is similar to the one in [13]. The SL is biased with a dc current and a lens is used to focus the emitted light on the external target. The OFSMI signal is detected by a monitor photodiode (PD) packaged in the rear of the SL, and is amplified by a trans-impedance amplifier. The amplified signal is then acquired by personal computer via an A/D card. Considering the case that the target is on simple harmonic vibration, we have

$$L(n) = L_0 + \Delta L_0 \sin \left(\frac{2\pi f n}{f_s} + \theta_0 \right) \quad (1)$$

where $L(n)$ is the distance between the laser facet and the external target, L_0 is the distance when the target is at the equilibrium position of the vibration, ΔL_0 is vibration amplitude, f is the vibration frequency, f_s is the sampling frequency of the A/D card, n is discrete time index, and θ_0 is the initial phase of the vibration at time $n = 0$, respectively.

The OFSMI effect has been studied extensively [18], [19] and a well known model describing the behavior has been developed [12]–[16], which shows that with existence of external target forming an external cavity of length L , the emitted laser power is given by

$$P(L) = P_0 [1 + mG(L)] \quad (2)$$

where P_0 is the intensity of the SL without external cavity. Equation (2) reveals that due to the external cavity, the emitted intensity deviates from P_0 by a factor of $mG(L)$ where m is the modulation index. The influence of the OFSMI effect on the emitted intensity is measured by $G(L)$, called the interference function, given by

$$G(L) = \cos(\Phi_F(L)) \quad (3)$$

and $\Phi_F(L)$ is the laser phase when the external target exists, which can be determined by:

$$\Phi_F(L) = \Phi_0(L) - C \cdot \sin[\Phi_F(L) + \arctan(\alpha)] \quad (4)$$

where $\Phi_0(L)$ is the laser phase without feedback under free running conditions, given by $\Phi_0(L) = 4\pi L/\lambda_0$, and where λ_0 is the emitted laser wavelength without feedback. Also in (4) C and α are the optical feedback level factor and the LEF, respectively. By combining (1)–(4) we have the following discrete model to describe the OFSMI considered above:

$$\phi_0(n) = A_0 + A \sin\left(\frac{2\pi f n}{f_s} + \theta_0\right) \quad (5)$$

$$\phi_F(n) = \phi_0(n) - C \cdot \sin[\phi_F(n) + \arctan(\alpha)] \quad (6)$$

$$g(n) = \cos(\phi_F(n)) \quad (7)$$

$$p(n) = P_0 [1 + m \cdot g(n)] \quad (8)$$

where $A_0 = 4\pi L_0/\lambda_0$ and $A = 4\pi\Delta L_0/\lambda_0$. Note that for the sake of simplicity we use $\phi_F(n) = \Phi_F(L(n))$, $\phi_0(n) = \Phi_0(L(n))$ and $g(n) = G(L(n))$. Also due to the cosine function in (7), $A_0 + 2k\pi$ for any integer k will yield the same $g(n)$. In other words, we are only able to identify A_0 up to $A_0 + 2k\pi$ where $A_0 \in [0, 2\pi]$ and k is an unknown integer. Therefore, in this paper we assume $A_0 \in [0, 2\pi]$.

When a block of the OFSMI signal samples $p(n)$ is acquired, we will firstly carry out pre-processing on the raw data, which removes P_0 and additive noise, and normalizes the amplitude. As the pre-processing will yield $g(n)$, we will treat $g(n)$ as the OFSMI signal based on which parameter estimation techniques will be developed.

III. DETERMINATION OF THE VIBRATION PARAMETERS

Equations (5)–(8) show that there are multiple parameters that influence the OFSMI signals, including not only α and C , but also the parameters associated with the external target vibration. We must take into account all the parameters although our primary aim is to estimate the LEF. In this section, we try to evaluate the parameters that can be individually estimated, including the vibration frequency, the rough value of vibration amplitude. We will also present an algorithm for automatic segmentation of the OFSMI data.

A. Estimation of the Vibration Frequency f

The vibration frequency f can be directly estimated from the OFSMI signal waveform regardless of other parameter values. As the external target is in harmonic vibration, from (5)–(7) we can see that $g(n)$ is also periodic and a fundamental period consists of N_0 data samples, where $N_0 = \text{int}[f_s/f]$ and where $\text{int}[\cdot]$ denotes the operation of taking the integer part of the number. Clearly the vibration frequency can be obtained by $f \approx f_s/N_0$. Hence, we can determine the period N_0 using the auto-correlation function as follows:

$$r_g(m) = \frac{1}{M} \sum_{n=0}^{M-1-m} g_M(n) \cdot g_M(n+m) \quad (9)$$

where M is number of data samples used for calculating the auto-correlation function. m is the time delay index which varies from $-(M-1)/2$ to $(M-1)/2$. As $g(n)$ has fundamental period N_0 , $r_g(m)$ should exhibit peaks at locations of integer multiples of N_0 and, hence, N_0 can be obtained

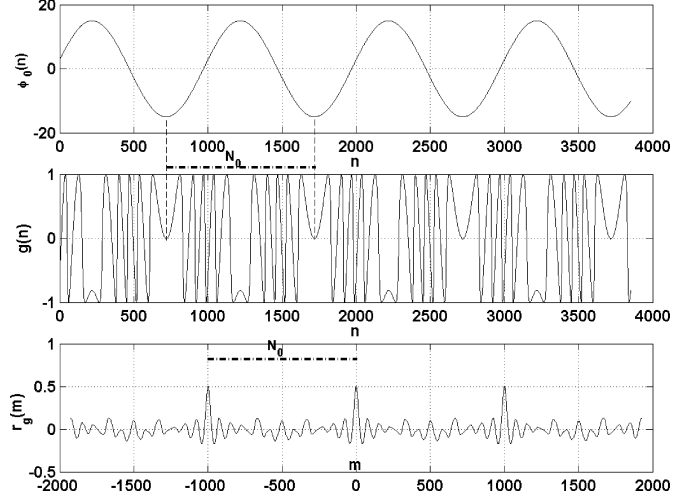


Fig. 2. Example of an vibration signal $\phi_0(n)$, the OFSMI signal $g(n)$, and the relevant autocorrelation $r_g(m)$.

by detecting the positions of the peaks in the auto-correlation function. As an example, Fig. 2 shows $\phi_0(n)$, the corresponding OFSMI signal, and its autocorrelation.

B. Segmentation of OFSMI Data—Determination of the Initial Phase θ_0

For realizing automatic measurement of LEF, segmentation of OFSMI data must be performed which divide the observed data stream into blocks. The data blocks are usually chosen in such a way that each block covers a whole cycle of vibration. As the period N_0 can be estimated by the technique described above, it is easy to choose data segments so that each segment contains N_0 samples or integer multiples of N_0 samples. In this situation, it is very important to know the instantaneous location of the external target when the first sample of the OFSMI data is taken for every data segment. Equivalently, the initial phase θ_0 must be known when a segment of OFSMI signal samples is taken from the data stream.

There are two ways to solve the issue. One is to randomly chose a segment of OFSMI data from the observed data stream based on which we try to determine the value of θ_0 . The other is to set up θ_0 to a specific value and then to choose the start point of the data segment. By studying the symmetrical property of the harmonic vibration and the OFSMI waveform, we find the later is easier which can be implemented as follows.

Let us rewrite (5) as follows:

$$\phi_0(n) = A_0 + A \sin\left(\frac{2\pi n}{N_0} + \theta_0\right). \quad (10)$$

If we choose $\theta_0 = -\pi/2$, $\phi_0(n)$ will exhibit the following symmetrical property within a fundamental period:

$$\phi_0(n) = \phi_0(N_0 - n), \quad \text{for } n = 0, 1, \dots, N_0 - 1. \quad (11)$$

As indicated by (6) and (7), there is a unique mapping relationship from $\phi_0(n)$ to $\phi_F(n)$ in the case of weak optical feedback where $C < 1$, and the mapping from $\phi_F(n)$ to $g(n)$ is also

unique. Hence, $g(n)$ should have the same symmetrical property, that is

$$g(n) = g(N_0 - n), \quad \text{for } n = 0, 1, \dots, N_0 - 1. \quad (12)$$

We can use (12) to locate the start point of the OFSMI data segment at which $\theta_0 = -\pi/2$. In other words, by choosing an OFSMI data block so that (12) is met, we will have $\theta_0 = -\pi/2$. This idea can be implemented as follows. When a stream of OFSMI data is obtained, we use a sliding window to pick up a segment of N_0 samples as follows:

$$g_w(n, j) = \begin{cases} g(n + j), & \text{for } n = 0, 1, \dots, N_0 - 1 \\ 0, & \text{otherwise} \end{cases} \quad (13)$$

where j is the starting point for the sliding window. The idea is to vary index j so that $g_w(n, j)$ satisfies condition in (12), that is, $g_w(n, j) = g_w(N_0 - n, j)$, for $n = 0, 1, \dots, N_0 - 1$. For this purpose we define the following cost function:

$$e(j) = \sum_{n=0}^{N_0-1} [g_w(n, j) - g_w(N_0 - n, j)]^2, \quad \text{for } j = 0, 1, \dots, \frac{N_0}{2} - 1. \quad (14)$$

By minimizing the above cost function with respect to the sliding window index j , we will obtain the OFSMI data block $g_w(n, j)$ that has the initial phase $\theta_0 = -\pi/2$.

IV. DATA-FITTING PRINCIPLE FOR ESTIMATIONS OF A , A_0 , C , AND α

Using the above approaches, we are now in a position to obtain the vibration frequency f , the initial phase θ_0 , as well as the rough value of A . We also are able to obtain OFSMI data blocks of N_0 data samples with known initial vibration phase θ_0 . As seen from (5)–(7) the remaining parameters still unknown are A , A_0 , C , and α .

Estimation of the above unknown parameters is challenging task as their influence to the OFSMI waveform is coupled together. Similar to the work in [13], we want to employ data-to-theoretical model fitting techniques. The idea is to choose parameter values with which the theoretical model yields an OFSMI signal waveform that are as close as possible to the observed experimental data. A straight forward way for data fitting is to minimize a cost function as follows:

$$F(\hat{A}, \hat{A}_0, \hat{C}, \hat{\alpha}) = \frac{1}{M} \sum_{n=1}^M [g(n) - \hat{g}(n, \hat{A}, \hat{A}_0, \hat{C}, \hat{\alpha})]^2 \quad (15)$$

where M is data length of $g(n)$ used for estimating the parameters, and in this paper we choose $M = N_0$ as each data segment contains N_0 data samples. $\hat{g}(n, \hat{A}, \hat{A}_0, \hat{C}, \hat{\alpha})$ ($n = 1, 2, \dots, M$) are the values based on computation using models in (5)–(7) incorporating the values of $(\hat{A}, \hat{A}_0, \hat{C}, \hat{\alpha})$. It is expected that minimization of the above cost function in (15) with respect to $(\hat{A}, \hat{A}_0, \hat{C}, \hat{\alpha})$ will yield accurate estimation of these parameters.

The cost function $F(\hat{A}, \hat{A}_0, \hat{C}, \hat{\alpha})$ plays a significant role for the performance of the parameter estimation. In order to yield unbiased estimates of the parameters, we hope that $F(\hat{A}, \hat{A}_0, \hat{C}, \hat{\alpha})$ has a global minimum corresponding to true parameter values. We also wish that the global minimum could be reached with a suitable optimization algorithm. As there are four parameters that may be coupled together in terms of their influence on the cost function, we must also have suitable strategy for carrying out the minimization of the cost function. For this purpose we should study $F(\hat{A}, \hat{A}_0, \hat{C}, \hat{\alpha})$ by looking at its surface shape with respect to $(\hat{A}, \hat{A}_0, \hat{C}, \hat{\alpha})$ in a multiple-dimensional space.

The surface shape of $F(\hat{A}, \hat{A}_0, \hat{C}, \hat{\alpha})$ with respect to \hat{C} and $\hat{\alpha}$ has been studied in [13] under the condition that A and A_0 are known. It was shown that $F(\hat{A}, \hat{A}_0, \hat{C}, \hat{\alpha})$ has one global minimum respect to \hat{C} and $\hat{\alpha}$ when $\hat{A} = A$ and $\hat{A}_0 = A_0$, and the global minimum is located where \hat{C} and $\hat{\alpha}$ take the true values. However, for the situations considered in this paper, A and A_0 are also unknown and so we should look at the characteristics of $F(\hat{A}, \hat{A}_0, \hat{C}, \hat{\alpha})$ with respect to all the parameters $(\hat{A}, \hat{A}_0, \hat{C}, \hat{\alpha})$.

Computer simulations are performed to study the surface shape of $F(\hat{A}, \hat{A}_0, \hat{C}, \hat{\alpha})$ with the following procedures. First, we set up a set of true parameter values (A, A_0, C, α) and use (5) to (7) to generate $g(n)$, which is considered as the OFSMI signal observed. Then by varying the estimated parameters $(\hat{A}, \hat{A}_0, \hat{C}, \hat{\alpha})$ we use (5) to (7) again to yield $\hat{g}(n, \hat{A}, \hat{A}_0, \hat{C}, \hat{\alpha})$. Finally we use (15) to obtain $F(\hat{A}, \hat{A}_0, \hat{C}, \hat{\alpha})$.

In order to fully investigate the cost function, we have run the simulations for all possible true values of (A, A_0, C, α) . For illustration purpose, we present the results for a typical case where the true parameter values likely appear in Fig. 1. The true parameter values are $C = 0.5$, $\alpha = 3.3$, $f = 195$ Hz, $f_s = 200$ kHz, $\Delta L_0 = 1 \mu\text{m}$ (thus $A = 16.1$ rad for $\lambda_0 = 780$ nm), and $L_0 = 24$ cm (thus $A_0 = 1.747$ rad for $\lambda_0 = 780$ nm), respectively. These true parameter values are used to create $g(n)$. As f and θ_0 are unknown in practice, we should still use the approach proposed in Sections III-A and B to determine their values. Also, as there are four parameters, we divide them into two groups and consider one group each time while leaving the other group constant.

A. Influence of $\hat{\alpha}$ and \hat{C} to the Cost Function

It is natural to see if the approach in [13] can be directly applied to the case when A_0 and A are unknown. For this purpose we look at the impact of $\hat{\alpha}$ and \hat{C} on the cost function as follows.

- First, we consider the case when \hat{A}_0 and \hat{A} take their true values, that are, $A = 16.1$ rad and $A_0 = 1.747$ rad. As shown in [13] the surface shape of $F(\hat{A}, \hat{A}_0, \hat{C}, \hat{\alpha})$ with respect to variance of $\hat{\alpha}$ and \hat{C} is unimodal, and that minimization of $F(\hat{A}, \hat{A}_0, \hat{C}, \hat{\alpha})$ with respect to $\hat{\alpha}$ and \hat{C} will yield good estimation of the parameters α and C .
- Then we look at $F(\hat{A}, \hat{A}_0, \hat{C}, \hat{\alpha})$ in the case when \hat{A}_0 and \hat{A} deviate from their true values. We found that the surface is complex and does not exhibit a minimum at the location of the true values of α and C . Therefore, the approach proposed in [13] can not be directly used when the true values of \hat{A}_0 and \hat{A} are not available. As an example, Fig. 3 shows the

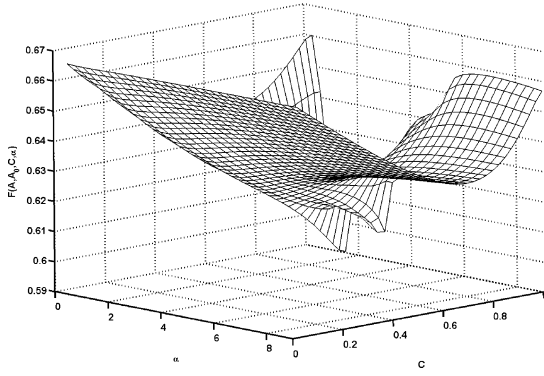


Fig. 3. Surface shape of the cost function with respect to variance of $\hat{\alpha}$ and \hat{C} when \hat{A}_0 and \hat{A} deviate from their true values A and A_0 . The simulation parameters are: $A = 16.1$, $A_0 = 1.747$; $\hat{A}_0 = 1.747 + 0.6$ and $\hat{A} = 16.1 + 1.9$.

cost function with respect to variance of $\hat{\alpha}$ and \hat{C} when $\hat{A}_0 = 1.747 + 0.6$ (rad) and $\hat{A} = 16.1 + 1.9$ (rad).

B. Influence of \hat{A}_0 and \hat{A} to the Cost Function

Now we consider the cost function with respect to \hat{A}_0 and \hat{A} . We also consider two situations as follows.

- First, we examine the case that $\hat{\alpha}$ and \hat{C} take their true values, that is, $\hat{\alpha} = \alpha = 3.3$ and $\hat{C} = C = 0.5$. Fig. 4(a) shows the surface shape of the cost function with respect to the variance of \hat{A}_0 and \hat{A} . We found that the surface is unimodal which exhibits a single minimum at the locations of the true values of \hat{A}_0 and \hat{A} . This result implies that when accurate values of $\hat{\alpha}$ and \hat{C} are available, optimization of the cost function with respect to \hat{A}_0 and \hat{A} will give unbiased estimation of the vibration amplitude.
- Next, let us consider the case where $F(\hat{A}, \hat{A}_0, \hat{C}, \hat{\alpha})$ is calculated using approximate values for $\hat{\alpha}$ and \hat{C} . Based on our extensive simulations using many different values of $\hat{\alpha}$ and \hat{C} , we found that the surface is always unimodal within a large area around a global minimum corresponding to the true values of \hat{A}_0 and \hat{A} . These results are very useful as they imply that even when true values of $\hat{\alpha}$ and \hat{C} are not available, by setting them to some approximate ones, optimization of the cost function with respect to \hat{A}_0 and \hat{A} still yields unbiased estimation of them. Also for illustration purpose, Fig. 4(b) shows the surface shape of the cost function with respect to variance of \hat{A}_0 and \hat{A} when $\hat{\alpha} = 5$ and $\hat{C} = 0.2$.

Based on the above results, we are able to propose a strategy to search for the parameter values, consisting of the following steps.

- Step 1) Setting $\hat{\alpha}$ and \hat{C} to some reasonable values (for example, if $0 < C < 1$ and $0 < \alpha < 10$, it is reasonable to choose $\hat{C} = 0.6$ and $\hat{\alpha} = 5$), we minimize the cost function with respect to \hat{A}_0 and \hat{A} . Based on the analysis above this will yield unbiased estimation of (A, A_0) .
- Step 2) Using the estimated \hat{A}_0 and \hat{A} from Step 1, we minimize the cost function again with respect to $\hat{\alpha}$ and \hat{C} in order to determine the values of both α and C .

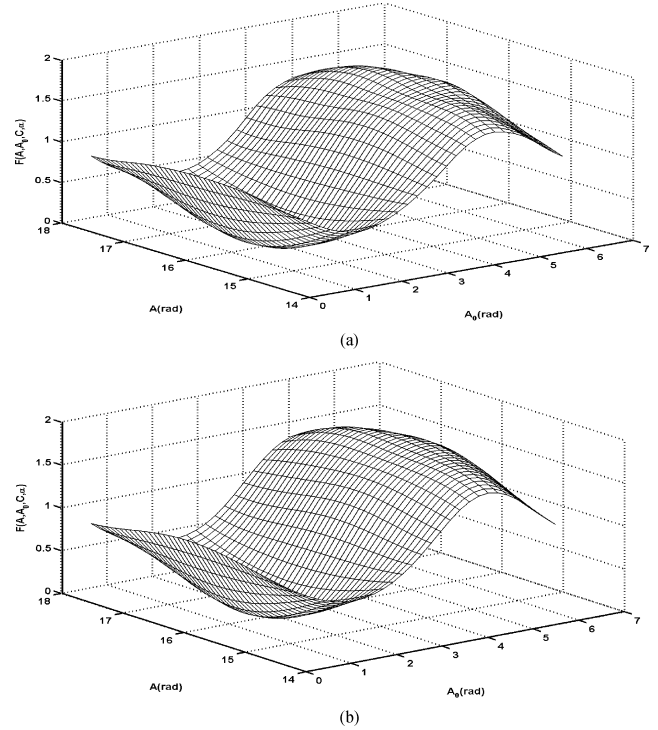


Fig. 4. Surface shape of the cost function with respect to variance of \hat{A}_0 and \hat{A} . The simulated parameters are (a) $\hat{\alpha} = \alpha = 3.3$ and $\hat{C} = C = 0.5$ and (b) $\alpha = 3.3$, $C = 0.5$, and $\hat{\alpha} = 5$, $\hat{C} = 0.2$.

The two steps can be run repetitively until the estimated parameters reach stable solutions. An approach for performing the minimization will be detailed in the following sections.

V. MINIMIZATION OF THE COST FUNCTION USING GRADIENT-BASED ALGORITHM

Various optimization techniques can be used to achieve minimization of the cost function using the procedure described in Section IV. In this paper we still use the gradient-based algorithm. The idea is that, starting from a set of initial values chosen, the parameters are updated toward the direction in which $F(\hat{A}, \hat{A}_0, \hat{C}, \hat{\alpha})$ exhibits fastest decrease. The iteration equations are shown in (16)–(19) at the bottom of the next page, where $\mu_A, \mu_{A_0}, \mu_C, \mu_\alpha > 0$ which are the step sizes for updating the parameters, and the subscript j refers to the iteration index. $\Re(n) = 1/(1 + \hat{C} \cos[\hat{\phi}_{Fj-1}(n) + \arctan \hat{\alpha}])$.

Equations (16)–(19) are the algorithms to update the parameters in order to yield the best data fitting. Note that compared to the gradients presented in [13], the ones in (18) and (19) are more accurate. There was a minor mistake in [13], where $\Re(n)$ and $\Re(n)/(1 + \hat{\alpha}^2)$ were missed.

In order to achieve best convergence performance, the following issues must be taken into account. First, the initial parameter values should be chosen within a reasonable range. As \hat{A} can be roughly estimated by the approach in Section III, we will use the result as the initial value. Also as $0 \leq \hat{A}_0 \leq 2\pi$, $0 < C \leq 1$, and $0 < \alpha \leq 10$, we can choose π , 0.6, and 5 as the initial values for \hat{A}_0 , C and α , respectively. Second, the parameters should be updated in a proper order. As discussed in Section IV, we should update \hat{A}_0 and \hat{A} first, and then update

TABLE I
PROCEDURE FOR THE DATA PROCESSING

Step 1. Pre-process the signal $p(n)$ to get $g(n)$, including filtering, P_0 removal and normalization of the signal amplitude.
Step 2. Estimate N_0 (and $f = \frac{f_s}{N_0}$) using the algorithm in Section III A.
Step 3. Obtain the rough value of A by fringe counting.
Step 4. Use the sliding window approach in Section III C to divide the OFSMI data into segments, and each segment covers a whole vibration cycle with the initial phase $\theta_0 = -\frac{\pi}{2}$.
Step 5. For each of the segment obtained in Step 4, setting the initial values $\hat{A}_0 = \pi$, $\hat{A} = \pi N_{fringe}$, $\hat{C} = 0.6$ and $\hat{\alpha} = 5$, estimate the parameters according to the following steps:
Step 6. Use Equations (16) and (17) repetitively to estimate A_0 and A (and thus $\Delta L_0 = \frac{A\lambda_0}{4\pi}$).
Step 7. Incorporating the estimates of \hat{A}_0 and \hat{A} obtained from Step 6 in the cost function, use Equations (18) to (19) repetitively to estimate C and α .
Step 8. Go back to Step 6, using the estimated results from Steps 6 and 7 as initial values, update the estimations until stable results are achieved.
Step 9. Perform steps 5 to 8 for all the data segments, and average the results obtained, which are the final estimation results for the parameters.

\hat{C} and $\hat{\alpha}$. Finally, the step size μ_A , μ_{A_0} , μ_C and μ_α must be chosen with care. Generally speaking, bigger step size leads to faster convergence but unfortunately larger steady state errors. Hence, a judicious choice of the step sizes is required. The proposed approach can be summarized by the steps in Table I.

VI. ESTIMATING RESULTS

In order to test the proposed approach, we acquired streams of OFSMI data using the OFSMI system in Fig. 1. In the system we used a GaAlAs multi-quantum well (MQW) laser diode (LD), HL7851G manufactured by HITACHI. The LD is biased with a dc current of 90 mA and works at single mode with a central wavelength of $\lambda_0 = 780$ nm. The temperature is kept at $25 \pm 0.1^\circ\text{C}$ using a temperature controller. We use a piezo-electric transducer (PZT) actuator with preset vibration frequency and magnitude. In the experiment we made the PZT vibrate simple harmonically with the nominal frequency of 195 Hz and the amplitude of $1.0 \mu\text{m}$. These experiment conditions are kept unchanged throughout the experiment.

OFSMI data are observed and recorded using the OFSMI system described above. By adjusting the system, we acquired

TABLE II
MEASURED RESULTS ON THE VIBRATION PARAMETERS

Data file	Block 1	Block 2	Block 3
\hat{f} (Hz)	195.6	195.5	195.5
$\frac{\delta_f}{\hat{f}}$	0.04%	0.04%	0.04%
$\Delta \hat{L}_0$ (nm)	1005.3	1003.7	1004.8
$\frac{\delta_{\Delta L_0}}{\Delta \hat{L}_0}$	0.14%	0.26%	0.22%

many blocks of OFSMI signals, each corresponding to a different C level. For each data block, parameters are estimated following the procedure in Table I. Also note that in Step 4, each

$$\hat{A}_j = \hat{A}_{j-1} - 2\mu_A \sum_{n=1}^N [g(n) - \hat{g}(n, \hat{A}_{j-1}, \hat{A}_{0j-1}, \hat{C}_{j-1}, \hat{\alpha}_{j-1})] \times \sin(\hat{\phi}_{Fj-1}(n)) \cdot \sin\left(\frac{2\pi n}{N_0}\right) \times \Re(n) \quad (16)$$

$$\hat{A}_{0j} = \hat{A}_{0j-1} - 2\mu_{A_0} \sum_{n=1}^N [g(n) - \hat{g}(n, \hat{A}_{j-1}, \hat{A}_{0j-1}, \hat{C}_{j-1}, \hat{\alpha}_{j-1})] \times \sin(\hat{\phi}_{Fj-1}(n)) \times \Re(n) \quad (17)$$

$$\hat{C}_j = \hat{C}_{j-1} + 2\mu_C \sum_{n=1}^N \left\{ g(n) - \hat{g}(n, \hat{A}_{j-1}, \hat{A}_{0j-1}, \hat{C}_{j-1}, \hat{\alpha}_{j-1}) \right\} \times \sin(\hat{\phi}_{Fj-1}(n)) \sin[\hat{\phi}_{Fj-1}(n) + \arctan \hat{\alpha}] \times \Re(n) \quad (18)$$

$$\hat{\alpha}_j = \hat{\alpha}_{j-1} + 2\mu_\alpha \hat{C}_j \sum_{n=1}^N \left\{ g(n) - \hat{g}(n, \hat{A}_{j-1}, \hat{A}_{0j-1}, \hat{C}_{j-1}, \hat{\alpha}_{j-1}) \right\} \times \sin(\hat{\phi}_{Fj-1}(n)) \cdot \cos[\hat{\phi}_{Fj-1}(n) + \arctan \hat{\alpha}] \times \frac{\Re(n)}{1 + \hat{\alpha}^2} \quad (19)$$

TABLE III
ESTIMATION RESULTS USING THE PROPOSED APPROACH IN COMPARISON WITH THE APPROACHES IN [12] AND [13]: DATA BLOCKS 1–3 ARE OBTAINED AT WEAK OPTICAL FEEDBACK, AND DATA BLOCKS 4–6 ARE OBTAINED AT MODERATE OPTICAL FEEDBACK

Data file	Block1		Block2		Block3		Block4	Block5	Block6
Approaches	This paper	[13]	This paper	[13]	This paper	[13]	[12]	[12]	[12]
$\hat{\alpha}$	3.320	3.512	3.237	3.279	3.288	3.349	3.417	3.265	3.180
$\delta_{\hat{\alpha}}/\hat{\alpha}$	5.71%	6.70%	3.39%	5.80%	4.64%	6.07%	10.02%	7.05%	6.17%

OFSMI data block was divided into ten segments and the final estimation is obtained by averaging the results from all the ten segments.

For comparison purposes, we also applied the approach in [13] to each of data blocks. As the movement trace must be known when using the approach in [13], we used the nominal frequency of 195 Hz and the amplitude of 1.0 μm , respectively, and manually performed the data segmentation. In addition, we tested the same LD with the approach in [12] in order to further compare the performance.

The measurement results are summarized in Tables II and III, respectively, where \hat{f} , $\Delta\hat{L}_0$ ($\Delta\hat{L}_0 = \hat{A}\lambda_0/4\pi$) and $\hat{\alpha}$ are the estimated parameter values, respectively. We calculated the relative standard deviation of the estimation results for each OFSMI signal block, given by δ_f/\hat{f} , $\delta_{\Delta L_0}/\Delta\hat{L}_0$ and $\delta_{\hat{\alpha}}/\hat{\alpha}$, where δ_f , δ_{L_0} , $\delta_{\Delta L_0}$ and $\delta_{\hat{\alpha}}$ are the standard deviation of the estimated results from their averages. The standard deviations can evaluate the consistency of the measurement. As the analysis in Section IV shows that the proposed cost function exhibit global minimum corresponding to the true parameter values, it is expected that the estimation results are unbiased. In this case, smaller standard deviations imply higher estimation accuracy. Note that we did not display the estimated L_0 in Table II, as the external target was placed at different positions when acquiring the three signal blocks, and also L_0 can only be determined within $[0, 2\pi]$ plus a unknown integer multiples of $[0, 2\pi]$.

Table II shows the estimated results for the vibration frequency and amplitude, respectively, using the approaches in Sections II and III. The results show that these estimations are effective as they are close to the nominal values and the standard deviations are very small. Table III gives the results for the LEF obtained from the three approaches mentioned above. It is seen that the results are very close, which is reasonable as the LEF should be constant for the same LD. Also we noticed that the results by the proposed approach have lower relative standard deviation, implying more accurate as the estimations are unbiased. This may result from the use of more accurate gradients, and the real-time estimation of $\Delta\hat{L}_0$ which is more accurate in contrast to [13] in which $\Delta\hat{L}_0$ is determined in advance and considered as a constant, implying that the fluctuation in time is ignored. Besides, both the proposed approach and [13] have a smaller standard deviation than [12], which indicates that the data fitting techniques for OFSMI with weak optical feedback are more robust as it does not suffer from the problems such as nonlinear feedback phase and measurement noise.

The above measurement results would be more convincing if they can be compared to the LEF value of the same LD given

by the manufacture or by other measurement methods. Unfortunately, we were not able to do so as the LEF for the LD is not specified by the maker and we do not have the experiment setup required for other methods except for the method in [12]. However, comparisons among nine different techniques, including the one in [12], have been conducted in [20]. It shows [20] that for the same laser, the approach in [12] yields LEF value that is consistent with other approaches. Therefore, given the consistency of the measurement results shown in Table III, we may be able to say that the proposed approach provides an effective and accurate way to measure the LEF.

VII. CONCLUSION

This paper presented an optimized strategy to achieve estimation of all the parameters in an OFSMI system with an external target on simple harmonic vibration. Theoretical and simulation analysis shows that the estimations are unbiased. Test with experimental data shows that the proposed approach is able to achieve the measurement of LEF with the standard deviation of less than 4.58% on average. Compared to existing approaches in this area, such as [12] and [13], the proposed approach has the following advantageous contributions. First, the proposed approach does not need to know the exact movement trace of the external target, which is obviously more useful in practice than the technique proposed in [13] where the exact movement trace must be known *a priori*. Second, the proposed approach does not require a constant speed of external target and, hence, it does not suffer from the inherent error associated with the approach in [12]. In addition, the proposed approach is based on the principle of data-to-model fitting and signal processing and so it keeps the advantages of the approach in [13] in terms of increased robustness and noise immunization as compared to [12]. Moreover, the approach can be implemented in an automatic manner in that when a stream of OFSMI data is acquired, the data stream can be automatically divided into segments, based on which parameter estimation can be implemented. Finally, the approach also provides a way to measure parameters associated with external target vibration, including frequency and magnitude, which have many other potential applications.

REFERENCES

- [1] M. W. Fleming and A. Mooradian, "Fundamental line broadening of single-mode (GaAl)As diode lasers," *Appl. Phys. Lett.*, vol. 38, no. 7, pp. 511–513, 1981.
- [2] C. H. Henry, R. A. Logan, and K. A. Bertness, "Spectral dependence of the change in refractive index due to carrier injection in GaAs lasers," *J. Appl. Phys.*, vol. 52, no. 7, pp. 4457–4461, 1981.

- [3] M. Osinski and J. Buus, "Linewidth broadening factor in semiconductor lasers—An overview," *IEEE J. Quantum Electron.*, vol. 23, no. 1, pp. 9–29, Jan. 1987.
- [4] H. R. Choo, O. Beom-hoan, C. D. Park, H. M. Kim, J. S. Kim, D. K. n. Oh, H. M. Kim, and K. E. Pyun, "Improvement of linewidth enhancement factor in 1.55- μm multiple-quantum-well laser diodes," *IEEE Photon. Technol. Lett.*, vol. 10, no. 5, pp. 645–647, May 1998.
- [5] T. B. Simpson, F. Doft, E. Strzelecka, J. J. Liu, W. Chang, and G. J. Simonis, "Gain saturation and the linewidth enhancement factor in semiconductor lasers," *IEEE Photon. Technol. Lett.*, vol. 13, no. 8, pp. 776–778, Aug. 2001.
- [6] H. Halbritter, F. Riemenschneider, J. Jacquet, J.-G. Provost, C. Symonds, I. Sagnes, and P. Meissner, "Chirp and linewidth enhancement factor of tunable, optically-pumped long wavelength VCSEL," *Electron. Lett.*, vol. 40, no. 4, pp. 242–244, Feb. 2004.
- [7] P. K. Kondratko, S. L. Chung, and N. Holonyak, "Observations of near-zero linewidth enhancement factor in a quantum-well coupled quantum-dot laser," *Appl. Phys. Lett.*, vol. 83, no. 6, pp. 4818–4820, Dec. 2003.
- [8] H. Li, "RF-modulation measurement of linewidth enhancement factor and nonlinear gain of vertical-cavity surface-emitting lasers," *IEEE Photon. Technol. Lett.*, vol. 8, no. 12, pp. 1594–1596, Dec. 1996.
- [9] G. Liu, X. Jin, and S. L. Chuang, "Measurement of linewidth enhancement factor of semiconductor lasers using an injection-locking technique," *IEEE Photon. Technol. Lett.*, vol. 13, no. 5, pp. 430–432, May 2001.
- [10] K. E. Chlouverakis, K. M. Al-Aswad, I. D. Henning, and M. J. Adams, "Determining laser linewidth parameter from Hopf bifurcation minimum in lasers subject to optical injection," *Electron. Lett.*, vol. 39, no. 16, pp. 1185–1187, Aug. 2003.
- [11] Y. S. Shin, T. H. Yoon, J. R. Park, and C. H. Nam, "Simple methods for measuring the linewidth enhancement factor in external cavity laser diodes," *Opt. Commun.*, vol. 173, pp. 303–309, Jan. 2000.
- [12] Y. Yu, G. Giuliani, and S. Donati, "Measurement of the linewidth enhancement factor of semiconductor lasers based on the optical feedback self-mixing effect," *IEEE Photon. Technol. Lett.*, vol. 16, no. 4, pp. 990–992, Apr. 2004.
- [13] J. Xi, Y. Yu, J. Chicharo, and T. Bosch, "Estimating the parameters of semiconductor lasers based on weak optical feedback interferometry," *IEEE J. Quantum Electron.*, vol. 41, no. 8, pp. 1058–1064, Aug. 2005.
- [14] G. Giuliani, M. Norgia, S. Donati, and T. Bosch, "Laser diode self-mixing technique for sensing applications," *J. Opt. A: Pure Appl. Opt.*, vol. 4, no. 6, pp. S283–S294, 2002.
- [15] S. Donati, G. Giuliani, and S. Merlo, "Laser diode feedback interferometer for measurement of displacements without ambiguity," *IEEE J. Quantum Electron.*, vol. 31, no. 1, pp. 113–119, Jan. 1995.
- [16] L. Scalise, Y. Yu, G. Giuliani, G. Plantier, and T. Bosch, "Self-mixing laser diode velocimetry: Application to vibration and velocity measurement," *IEEE Trans. Instrum. Meas.*, vol. 53, no. 1, pp. 223–232, Jan. 2004.
- [17] G. A. Acket, D. Lenstra, A. J. D. Boef, and B. H. Verbeek, "The influence of feedback intensity on longitudinal mode properties and optical noise in index-guided semiconductor lasers," *IEEE J. Quantum Electron.*, vol. QE-20, no. 10, pp. 1163–1169, Oct. 1984.
- [18] R. Lang and K. Kobayashi, "External optical feedback effects on semiconductor injection laser properties," *IEEE J. Quantum Electron.*, vol. QE-16, no. 3, pp. 347–355, Mar. 1980.
- [19] N. Schunk and K. Pertermann, "Numerical analysis of the feedback regimes for a single-mode semiconductor laser with external feedback," *IEEE J. Quantum Electron.*, vol. 24, no. 7, pp. 1242–1247, Jul. 1988.
- [20] T. Fordell and A. M. Lindberg, "Experiments on the linewidth enhancement factor of a vertical-cavity surface-emitting laser," *IEEE J. Quantum Electron.*, vol. 43, no. 1, pp. 6–15, Jan. 2007.



Yanguang Yu received the Ph.D. degree in precision instruments and mechanisms from the Harbin Institute of Technology, Harbin, China, in 2000.

She is currently a Professor at the College of Information Engineering, Zhengzhou University, Zhengzhou, China. From 2001 and 2002, she was a Postdoctoral Fellow at Opto-Electronics Information Science and Technology Laboratory, Tianjin University, China. She had a number of visiting appointments including a Visiting Fellow at the Optoelectronics Group, Department of Electronics,

University of Pavia, Italy (2002–2003), a Principal Visiting Fellow at the School of Electrical Computer and Telecommunications Engineering, the University of Wollongong, Australia (2004–2005), a visiting Associate Professor and Professor in the Engineering School ENSEEIHT, Toulouse, France, in 2004 and 2006, respectively. Her research interests include semiconductor lasers with optical feedback and optical feedback interferometry and their applications to instrumentation and measurement.



Jiangtao Xi (M'95–SM'06) received the B.Eng. degree from Beijing Institute of Technology, Beijing, China, in 1982, the M.Eng. degree from TsingHua University, TsingHua, China in 1985, and the Ph.D. from the University of Wollongong, Wollongong, Australia, in 1996, all in electrical engineering.

He was a Postdoctoral Fellow at the Communications Research laboratory, McMaster University, Hamilton, ON, Canada from 1995 to 1996, a Member of Technical Staff at Bell Laboratories, Lucent Technologies Inc., Holmdel, NJ, from 1996 to 1998. He was the Chief Technical Officer at TCL IT Group Co., China, from 2000 to 2002. He rejoined the University of Wollongong, Wollongong, Australia, as a Senior Lecturer in 2003 and is currently an Associate Professor. His research interests are signal processing and its applications in various areas including photonics, optical electronics, and telecommunications.



Joe F. Chicharo (M'89–SM'94) received the B.E. degree (first-class hon.) and the Ph.D. degree from the University of Wollongong, Wollongong, Australia, in 1983 and 1990, respectively, both in electrical engineering.

He has been with the University of Wollongong, Wollongong, Australia, since 1985 as a Lecturer (1985–1990), Senior Lecturer (1990–1993), Associate Professor (1994–1997) and Professor (1997). From 2000 to 2003, he was the Research Director of an Australian Collaborative Research Center on Smart Internet Technology. He is currently the Dean of The Faculty of Informatics. His research interests are in the areas of digital signal processing, telecommunications, and engineering.

Thierry Bosch (M'93–SM'06) is currently Professor in the Engineering School, Ecole Nationale Supérieure d'Electrotechnique, d'Electronique, d'Informatique, d'Hydraulique et des Télécommunications (ENSEEIHT), Toulouse, France, and Director of Electronics Laboratory of ENSEEIHT (LEN7).

His research interests are related to laser industrial instrumentation development including range finding techniques, vibration and velocity measurements. He has cooperated in several programs of research and development with European companies active in the areas of sensor design, metrology, transportation, or avionics. He edited *Selected Papers on Laser Distance Measurements* (SPIE, 1995).

Dr. Bosch has created the International Conference ODIMAP and has been Guest co-Editor for *Journal of Optics* (June 1998, November 2002) and *Optical Engineering* (January 2001) on Distance/Displacement Measurements by Laser Techniques. Moreover, with Prof. Marc Lescure. He is currently the Chairman of the IEEE Instrumentation and Measurement Technical Committee "Lasers and Optical Systems" and has been an Associate Editor of the IEEE TRANSACTIONS ON INSTRUMENTATION AND MEASUREMENT since 1997.